29. A. R. Mazzeo and G. C. Levy, *Comput. Enhanced Spectrosc.* **3**, 165, (1986).
30. A. A. Bothner-By and J. Dadok, *J. Magn. Reson.* **72**, 540 (1987).
31. M. A. Delsuc and G. C. Levy, *J. Magn. Reson.* **76**, 306 (1988).
32. A. R. Mazzeo, M. A. Delsuc, A. Kumar, and G. C. Levy, *J. Magn. Reson.* **81**, 512-519 (1989).
33. H. Barkhuusen, R. De Beer, W. M. M. J. Bovée, and D. Van Ormondt, *J. Magn. Reson.* **61**, 465 (1985).
34. J. Tang and J. R. Norris, *J. Magn. Reson.* **69**, 180 (1986).
35. J. Tang and J. R. Norris, *J. Chem. Phys.* **84**, 5210 (1986).
36. A. E. Schussheim and D. Cowburn, *J. Magn. Reson.* **71**, 371 (1987).
37. H. Gesmar and J. J. Led, "Spectral Estimation of Two-dimensional NMR Signals Applying Linear Prediction to Both Dimensions", Thesis, Univ. of Copenhagen (1987).
38. F. Ni and H. A. Scheraga, *J. Magn. Reson.* **70**, 506 (1987).
39. M. A. Delsuc, F. Ni, and G. C. Levy, *J. Magn. Reson.* **73**, 548 (1987).
40. G. L. Bretthorst, "Bayesian Spectrum Analysis and Parameter Estimation", Ph.D. thesis, Department of Physics, Washington University, St. Louis, Missouri, August (1987).
41. E. T. Jaynes, in "Maximum-Energy and Bayesian Spectral Analysis and Estimation Problems", C. R. Smith and G. J. Erickson, eds., p. 1, Reidel, Dordecht, Holland (1987).
42. G. L. Bretthorst, C. C. Hung, D. A. D'Avignon, and J. J. H. Ackerman, *J. Magn. Reson.* **79**, 369-376 (1988).
43. J. H. Holland, K. J. Holyoad, R. E. Nisbett, and P. R. Thagard, *Induction: Process of Inference, Learning and Discovery* The MIT Press (1986).



# APPLICABILITY AND LIMITATIONS OF THREE-DIMENSIONAL NMR SPECTROSCOPY FOR THE STUDY OF PROTEINS IN SOLUTION[1]

Rolf Boelens[a], Christian Griesinger[b], Lewis E. Kay[c], Dominique Marion[d], and Erik R.P. Zuiderweg[e,f]

[a]Department of Chemistry
University of Utrecht
Padualaan 8
3584 CH Utrecht, The Netherlands
[b]Institute for Organic Chemistry
Johann Wolfgang Goethe University
Niederurseler Hang
6000 Frankfurt-am-Main 50
Federal Republic of Germany
[c]Laboratory of Chemical Physics
Bld. 2, NIDDK, National Institutes of Health
Bethesda, MD 20892, USA
[d]Centre de Biophysique Moleculaire
C.N.R.S.
F-45071 Orleans Cedex 2, France
[e]Pharmaceutical Discovery
Abbott Laboratories
Abbott Park, IL 60064, USA
[f]Present address:
Biophysics Research Division
University of Michigan
2200 Bonisteel Blvd.
Ann Arbor, MI 48109, USA

*Computational Aspects of the Study of Biological Macromolecules by Nuclear Magnetic Resonance Spectroscopy,* Edited by J.C. Hoch *et al.,* Plenum Press, New York, 1991

## ABSTRACT

Assignment procedures for backbone resonances of proteins are outlined for homonuclear and heteronuclear three-dimensional NMR spectroscopy. Phasecycling procedures in fast 3D experiments are discussed. Examples of data space reducing processing techniques are given. A new triple resonance based assignment procedure for protein resonances is outlined. The general advantages and disadvantages of homonuclear and heteronuclear three-dimensional NMR spectroscopy are discussed.


## INTRODUCTION (E.R.P. Zuiderweg)

The determination of the three-dimensional structures of small biomolecules (MW <10,000) in solution by two dimensional (2D) NMR spectroscopy has become a well established technique (for a review see ref. 1). The protocol consists of the assignment of the resonances of the proton NMR spectrum by scalar-correlated spectroscopy (COSY, DQF-COSY, TOCSY/HOHAHA), followed by the identification of nuclear Overhauser effect cross peaks between the resonances of sequentially adjacent structural units (amino acids, bases, or monosaccharides) from 2D NOE spectra. This assignment forms the basis of the subsequent search for NOE distance constraints between sequentially remote protons using 2D NOE spectra. The obtained NOE constraints are then used in structure calculation programs to obtain an ensemble of structures compatible with the NMR data.

This approach breaks down for larger systems, mainly because of the overlap problems in the 2D data sets caused by the larger number of resonances. This overlap interferes with unambiguous analysis. At the time two-dimensional NMR was developed, it was already realized that extension of the methods into more dimensions would lead to additional resolution[2]; just as two-dimensional spectra are better resolved than one-dimensional spectra, so are three-dimensional (3D) spectra better resolved than two-dimensional datasets. Thus, the above mentioned problem of overlapping resonances for larger systems can in principle be resolved by three dimensional (3D) spectroscopy. 3D NMR experiments are constructed by recording a series of 2D experiments as a function of another 2D experiment[3] as shown in Fig. 1.

The first reports on 3D NMR combined two homonuclear (proton) experiments such as COSY with COSY, NOESY with COSY, COSY with J-spectroscopy[3,4,4b]. These pioneering experiments showed that 3D NMR was practical and that the large amount of data involved could be handled properly; early applications of these homonuclear 3D experiments (NOESY with HOHAHA[5,6]) on proteins were published in 1988. A second approach to 3D NMR was demonstrated quickly thereafter, by combining a heteronuclear correlation experiment such as HMQC with a homonuclear experiment such as NOESY[7]. These experiments have the advantage that only large inter-



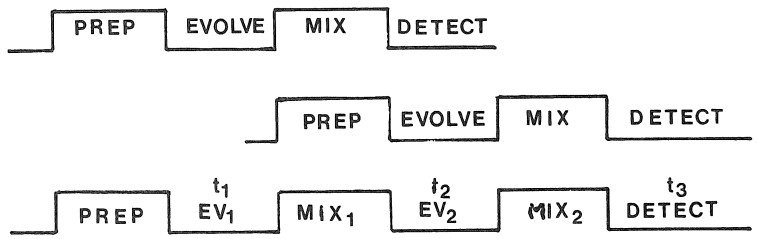


Figure 1. The construction of a three dimensional NMR experiment from two two-dimensional NMR experiments. The data are acquired during $t_3$ as a function of a matrix of $t_1$ and $t_2$ time variables, which are incremented independently.

actions are involved in the coherence transfer steps, which make them very suitable for larger systems, but have the disadvantage that the biomolecules need to be isotopically enriched. The application of heteronuclear 3D experiments to proteins ($^{15}$N labeled) was demonstrated in the next year[8,9]. A homonuclear 3D experiment suitable for the studies of larger proteins (NOE-NOE) was developed in the same year[10]. In the first half of 1990, the problem of the effect of the larger linewidth for larger systems on coherence transfer efficiency was addressed by redirecting these transfers over the $^{13}$C backbone[11,12], protein NOE spectra were resolved with respect to $^{13}$C[13,14], the first 4D experiment appeared[15], and an alternative assignment protocol for $^{13}$C, $^{15}$N labeled proteins was described[16,17].

To date, 3D NMR methods have been applied to Staphylococcal Nuclease, C5a, T4-lysozyme, Calmodulin, Interleukin 1 $\beta$, Rnase, Cyclophylin, Purotoxin, pike parvalbumin, Carbohydrates and DNA fragments. These rapid applications were possible because several problems associated with the recording, processing and interpretation of 3D NMR data could be solved (more versatile pulse-programmers, larger disks, faster computers, and advances in the biotechnology of isotopic labeling). The following reports describe some of these aspects, several issues that have not been solved to-date, and give an overview of the current state-of-the-art in 3D spectroscopy.

## PROTEIN SEQUENTIAL ASSIGNMENT PROCEDURES IN HOMO- AND HETERONUCLEAR 3D NMR SPECTROSCOPY (C. Griesinger)

Homo- and heteronuclear 3D NMR spectroscopy[18] of biomacromolecules relies mainly on the fact that the resolution due to the display of three chemical shifts is increased compared to the resolution of 2D spectra. One prominent application of 3D spectra so far concerns sequential assignment of resonances. For this purpose it is of interest how the increased resolution of 3D spectra translates into higher reliability and less ambiguity in the sequential assignment process.

The assignment procedure in 2D spectra can be described in the following way. Given a chain of spins A,B,C,D,E which pairwise interact either via scalar or dipolar coupling, we will find by recording the appropriate 2D spectra the following cross peaks: $(\omega_1, \omega_2) = (\Omega_A, \Omega_B)$, $(\Omega_B, \Omega_C)$, $(\Omega_C, \Omega_D)$, and $(\Omega_D, \Omega_E)$. These successive cross peaks have each one chemical shift in common. Thus they are connected in the 2D spectrum/spectra by a one dimensional search. The procedure becomes ambiguous as soon as there is degeneracy in the 1D spectrum.

In three dimensions, the optimal combination of 3D experiments will produce the following chain of cross peaks: $(\omega_1, \omega_2, \omega_3) = (\Omega_A, \Omega_B, \Omega_C)$, $(\Omega_B, \Omega_C, \Omega_D)$, $(\Omega_C, \Omega_D, \Omega_E)$. Again, successive cross peaks can be connected by a one-dimensional search, however now keeping two frequency coordinates fixed when going from one cross peak to the next. Therefore this 3D assignment procedure only becomes ambiguous if there is overlap between pairs of resonances which is less likely than overlap between resonances themselves. Thus this is the optimal 3D assignment procedure. It is more robust against overlap than 2D assignment procedures.

Analysis of some often used 3D sequences in application for proteins reveals the following: The homonuclear sequence NOESY-TOCSY[5,6] can be applied in the optimal way for sequential assignment both for $\beta$ sheet (relying on the strong NOE between $H_i^\alpha/NH_{i+1}$ and the intraresidual NH, $H_\alpha$ coupling) or $\alpha$ helical (relying instead on the $NH_i$, $NH_{i+1}$ NOE) secondary structures. The chain of cross peaks is constituted for $\beta$-sheet by: $(\omega_1, \omega_2, \omega_3) = (NH_i, H_{i-1}^\alpha, NH_{i-1})$, $(H_{i-1}^\alpha, NH_i, H_i^\alpha)$, $(NH_{i+1}, H_i^\alpha, NH_i)$ and for $\alpha$-helix by: $(\omega_1, \omega_2, \omega_3) = (NH_i, NH_{i-1}, H_{i-1}^\alpha)$, $(NH_{i-1}, NH_i, H_i^\alpha)$, $(NH_{i+1}, NH_i, H_i^\alpha)$.

For heteronuclear sequences[7,18] like NOESY-hetero-COSY and TOCSY-hetero-COSY with $^{15}N/^{13}C$ enriched proteins the situation is more complicated. If $^{15}N$ enrichment alone is used, only for $\alpha$-helical secondary structures the optimal assignment procedure can be applied: $(\omega_1, \omega_2, \omega_3) = (NH_i, {}^{15}N_{i-1}, NH_{i-1})$, $(NH_{i-1}, {}^{15}N_i, NH_i)$, $(NH_{i+1}, {}^{15}N_i, NH_i)$. This is demonstrated by a chain of three cross peaks substantiating the Val54-Glu55-Ala56 moiety contained in one of the $\alpha$-helices of ribonuclease A in Fig. 2. If heteronuclear sequences should be applied, $\beta$-sheet secondary structures need for the ideal assignment procedure in addition to $^{15}N$ labeling also $^{13}C$ labels at least in the $C_\alpha$-positions to get the following chain of resonances from the altogether four combinations of NOESY or TOCSY with C,H-hetero-COSY or N,H-hetero-COSY: $(\omega_1, \omega_2, \omega_3) = T(H_i^\alpha, {}^{15}NH_i, NH_i)$, $T(H_i^\alpha, {}^{13}C_i, NH_i)$, $N(H_i^\alpha, {}^{13}C_i, NH_{i+1})$, $N(H_i^\alpha, {}^{15}N_{i+1}, NH_{i+1})$, $T(H_{i+1}^\alpha, {}^{15}NH_{i+1}, NH_{i+1})$. (TOCSY peaks are designated with a T, NOESY peaks with an N). These experiments have been successfully carried out for Ribonuclease H[19].



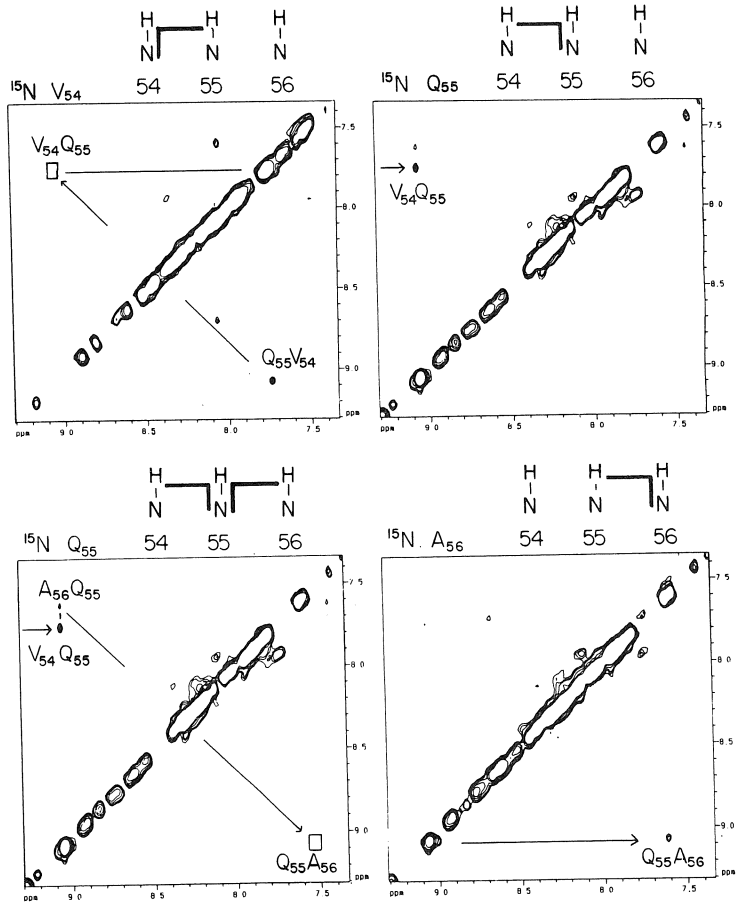


Figure 2. The sequential walk through the tripeptide moiety Val54-Glu55-Ala56 of ribonuclease A by a one-dimensional search is demonstrated in a NOESY-$^{15}$N,H-hetero-COSY experiment. $^{15}$N planes are shown together. The assignment of the respective cross peaks is given by a bar connecting the three correlated spins on the top of each spectrum. The NH resonance assignment is given in the spectra. Rectangles in the spectra designate positions of the type $(NH_i, {}^{15}N_i, NH_{i-1})$ which are obtained by reflection of the observable $(NH_{i-1}, {}^{15}N_i, NH_i)$ peaks at the $\omega_1 = \omega_3$ plane (C. Griesinger).

## DISCUSSION OF DR. GRIESINGER'S PAPER (E.R.P. Zuiderweg)

The general question of the sensitivity of homonuclear 3D NMR spectroscopy as compared to heteronuclear 3D NMR spectroscopy was raised by the moderator. The workers who co-authored the first (homonuclear) 3D experiment on a small protein (Drs. H. Oschkinat, C. Griesinger and G. M. Clore (ref. 5)), indicated that despite the relatively high concentration (6.8 mM), the NOESY-HOHAHA 3D spectrum of the small purotoxin protein was not entirely complete.

## HOMONUCLEAR 3D NMR OF BIOMOLECULES (R. Boelens)

Structure determination of biomolecules by NMR relies strongly on the observation of proton-proton NOE's[1]. First, they are essential in the so-called sequential assignment methods where neighbouring proton spin systems (often derived from proton J-coupling networks) are connected via unique NOE's at the polymer backbone. Secondly, most NMR methods for structure determination are based on proton-proton distance constraints, which can be derived from the NOE intensities. However, for large molecules (with a molecular weight above 10 kDa) the overlap of cross peaks in 2D NOE spectra even at high magnetic fields is already considerable, which complicates the assignment process and reduces the amount of observable distance constraints. Recently, both homo- and heteronuclear 3D NMR methods have been proposed to increase the resolution of the NMR spectra[4–9,20]. An advantage for the homonuclear technique is that no special isotope labeling of the biomolecular material is required. This makes it suitable for a broad range of biomolecules. Furthermore a single homonuclear 3D experiment can in principle contain all information required for both sequential and structural analysis. However, a clear disadvantage is that the mixing processes of homonuclear 3D, i.e., homonuclear J-coupling and cross relaxation, can cause inefficient magnetisation transfer. In addition, sequential assignment strategies based on only the proton-proton NOE can be ambiguous. Previously applications of homonuclear 3D NMR with proteins, oligosaccharides and DNA fragments have been given[21] and sequential assignment procedures based on 3D NOE-HOHAHA spectra have been developed[22,23].

### *A Non-Selective Homonuclear 3D Experiment*

For homonuclear 3D $^1$H NMR it seems very logical to combine a NOE and a HOHAHA experiment, since two important proton-proton interactions are now measured in one experiment. Fig. 3a shows the 3D NOE-HOHAHA pulse sequence, where the FID in the time domain $t_3$ is recorded as a function



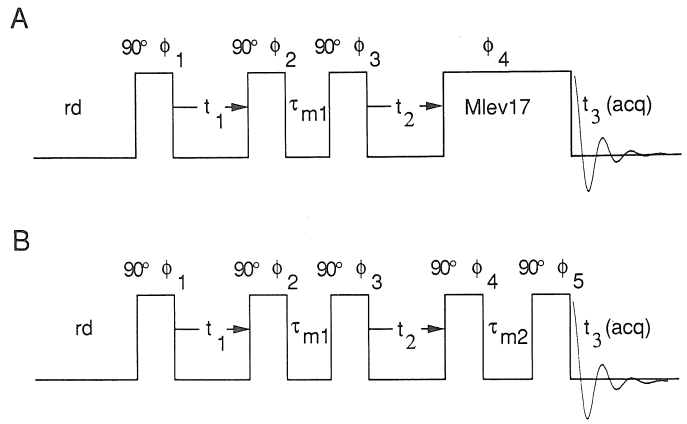


Figure 3. Pulse sequence for a 3D NOE-HOHAHA (a) and a 3D NOE-NOE experiment (b). MLEV-17 indicates the HOHAHA mixing sequence and $\tau_m$ corresponds to the NOE mixing time. Usually experiments with rf pulses with different phases are added (R. Boelens).

of two variable times $t_1$ and $t_2$. After Fourier transformation in the three dimensions a 3D spectrum is obtained with three independent frequency axes. A cross peak in this spectrum arises when magnetization of one proton is transferred in the first (NOE) mixing period to a second proton and then in the second (HOHAHA) mixing period to a third one. Since both the $t_1$ and $t_2$ time domains have to be incremented independently, a large number of FIDs are recorded in order to obtain a sufficiently high resolution for these two domains. In order to reduce measuring times and the amount of collected data it has been proposed to use semi-selective pulses which limit the spectral width to be sampled for the evolution domains[5,20]. However, in many cases such semi-selective or 'soft' pulses require additional phase cycling on a 180° echo pulse in order to obtain absorptive spectra. In that case a non-selective 3D NMR experiment which samples the full proton spectral width in all domains can be obtained in almost the same time and is therefore to be preferred. Measuring times can be reduced by minimal phase cycling schemes for reduction of artifacts. The HOHAHA mixing does not require any phase cycling to select the proper magnetization transfer and is therefore very suitable for 3D NMR. The NOE mixing requires no special phase cycling either, at least if a homospoil pulse can be given in the mixing time without interference with the spectrometer stability. If not, a choice must be made for SQC suppression (in a two-step phase cycle and generally sufficient for large biomolecules) or additional DQC suppression (in a four-step phase cycle). Suppression of axial peaks which develop in the evolution periods, can be accomplished by inversion of the first rf pulse combined with receiver switching. Often, imperfections of the instrument

demand dummy scans and additional phase cycling. In many cases these phases can be combined with the coherence suppression scheme. Thus, one FID in the 3D NOE-HOHAHA experiment can be recorded with one to 8 phases plus zero to two dummy scans. With 256 increments of both the $t_1$ and $t_2$ period and with a repetition rate of 1 s, this results in 18.2 to 182 hrs of measuring time.

### *A Single-Scan 3D NOE-NOE Experiment*

The miminal amount of scans per FID required for a non-selective 3D experiment is one. In order to test this we recorded a non-selective 3D NOE-NOE experiment of the protein parvalbumin (109 a.a.) in $^1H_2O$ with only a single scan. Coherences were suppressed by homospoil pulses in both NOE mixing times of 150 ms. The last rf pulse of the NOE-NOE pulse sequence was a semi-selective 45-$\tau$-45 pulse, which would not excite the $^1H_2O$ resonance. The quadrature image was eliminated from the 3D spectrum by positioning the rf carrier to the left of the amide region and discarding one half of the spectrum. Axial peaks were not suppressed, but there was sufficient space between the carrier and the spectrum to eliminate overlap. The loading of our instrument's pulse programmer together with the storage of the FID on disk caused an effective relaxation delay of 2.3 s. With 160*256 increments this resulted in 30 hrs measuring time. Fig. 4 shows a cross section perpendicular to $\omega_3$ through this 3D spectrum at 10.33 ppm. Comparison with a more traditional 3D NOE-NOE experiment recorded with 8 scans per FID and phase cycling, indicated that many 3D cross peaks can still be observed in this shorter experiment *cf.* Fig. 6). In fact, the S/N ratio was surprisingly good, probably due to limited sampling of $t_1/t_2$ noise in the short experimental time.

### *Analysis of Sequential and Medium Range Connectivities of a Protein by 3D NOE-HOHAHA and 3D NOE-NOE Spectroscopy*

Recently, we have analyzed the amide $\omega_3$ cross sections of the 3D HOHAHA-NOE spectrum of the protein parvalbumin in $^1H_2O$ and compared the sequential and medium range connectivities, which can be obtained from the 3D spectrum, with those extracted from 2D spectra[23]. The 3D spectrum allowed the observation of 455 3D cross peaks involving short and medium range NOE's, on which the assignment of 108 amino acids could be based. For the sequential contacts this is comparable to what was obtained previously from a whole series of 2D NOE spectra. In general, there were less $d_{NN}$ based NOEs observed, first because of the lower digital resolution which makes closely resonating protons indistinguishable and secondly because of the short $T_1$ and $T_2$ relaxation times of amide protons in the mixing and evo-



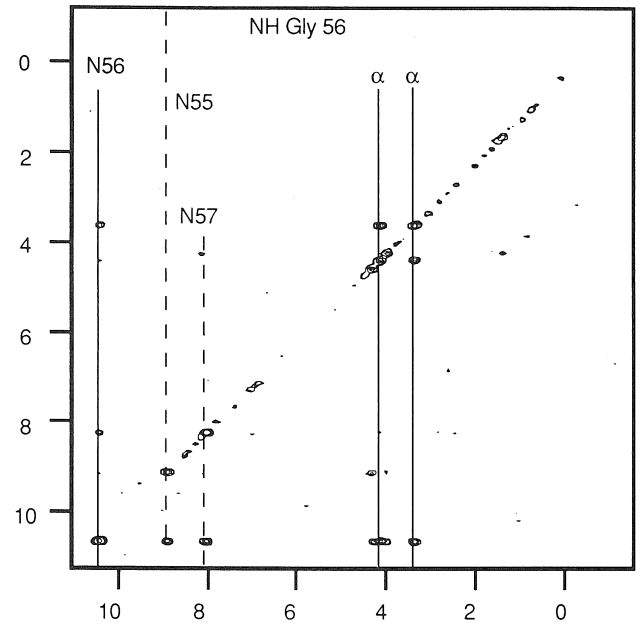


Figure 4. Cross section perpendicular to $\omega_3$ of a one-scan 3D NOE-NOE experiment of parvalbumin at the NH frequency of Gly 56 ($\omega_3$ = 10.33 ppm ). The spectrum was recorded at 500 Mhz with a 3D NOE-NOE sequence (*cf.* Fig. 3b) with a semi-selective 45-$\tau$-45 detection pulse and the rf carrier positioned to the left of the spectrum (R. Boelens).

lution periods which makes 3D cross peaks involving two amide protons most vulnerable. Fig. 5a summarizes the sequential and medium range connectivities which could be observed in a 3D HOHAHA-NOE experiment recorded with a 'clean' MLEV17 sequence[24] which gives a more efficient HOHAHA magnetization transfer. The 3D dataset allowed even a better definition of the secondary structure than was previously possible with 2D, since a series of new medium range NOE's were observed, mainly because the medium range $d_{\alpha\beta}$ and $d_{\alpha N}$ NOEs can be detected in non-overlapping regions. Furthermore, a preliminary analysis of the 3D 'clean' HOHAHA-NOE spectrum demonstrated that most long range NOE connectivities as obtained from 2D spectra could be found in the 3D spectrum as well (A. Padilla and R. Boelens, unpublished results). Of course, it should be realized that the analysis of the 3D HOHAHA-NOE spectra of parvalbumin was not an ab initio assignment, but was based on previous assignments obtained from 2D spectra. Until now we only showed that one 3D HOHAHA-NOE spectrum in principle contains all the information needed for assignment, secondary structure analysis and probably tertiary structure determination.

For large proteins the HOHAHA magnetization transfer in the 3D HOHAHA-NOE experiment could become inefficient in case of weakly coupled protons. Therefore, we have explored the feasibility of a homonuclear 3D

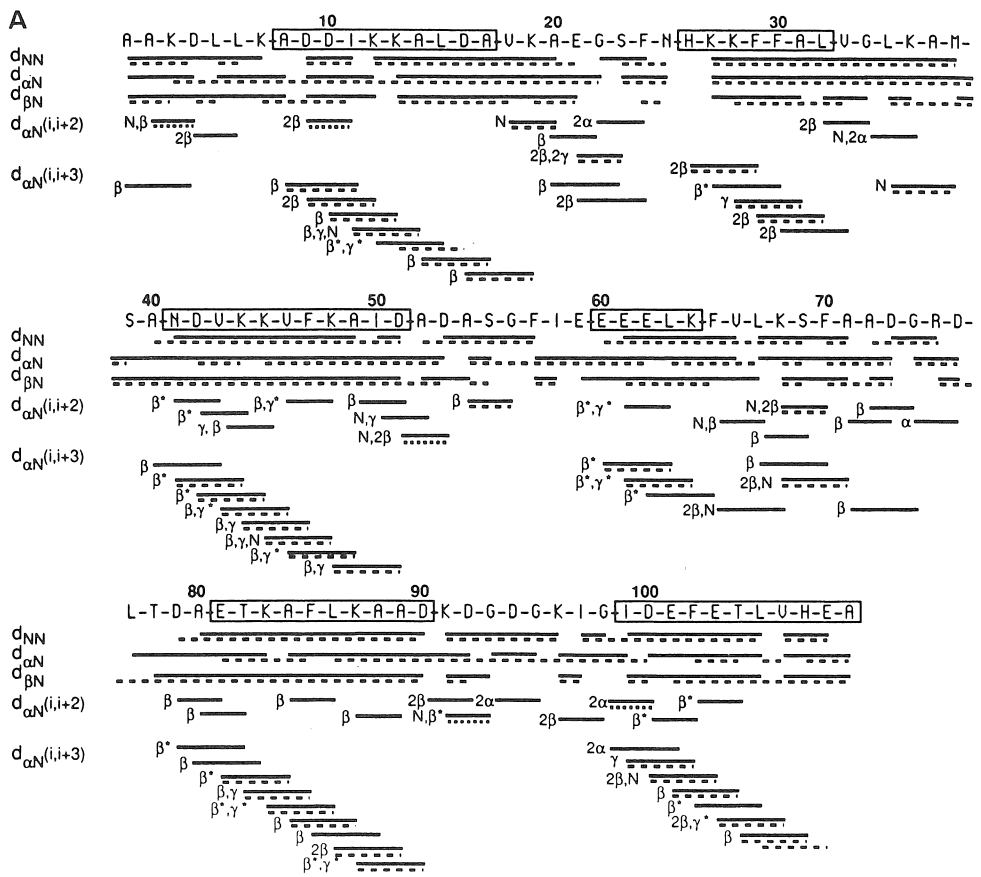


Figure 5. (a) Sequential and medium range NOEs in parvalbumin obtained from a 'clean' 3D HOHAHA-NOE spectrum (——) and those obtained from a set of 2D NOE spectra (- - - - - - - -).

technique that uses only NOE mixing periods[25]. We recorded a 3D NOE-NOE spectrum of parvalbumin in $^1H_2O$. Fig. 6 shows the corresponding cross sections from Ser 55 to Phe 57 in a 3D 'clean' HOHAHA-NOE spectrum and in a 3D NOE-NOE spectrum, demonstrating that sequential connectivities can be observed in both type of experiments. In fact most 3D connectivities identified in the 3D NOE-HOHAHA spectrum (Fig. 5a) can also be found in the 3D NOE-NOE spectrum (Fig. 5b). Although more complex for analysis, the 3D NOE-NOE spectrum can be used also for unraveling NOE patterns, as encountered in the sequential assignment of protein spectra. Since for large molecules cross relaxation becomes increasingly more efficient, the 3D NOE-NOE technique seems very suitable for large molecules.



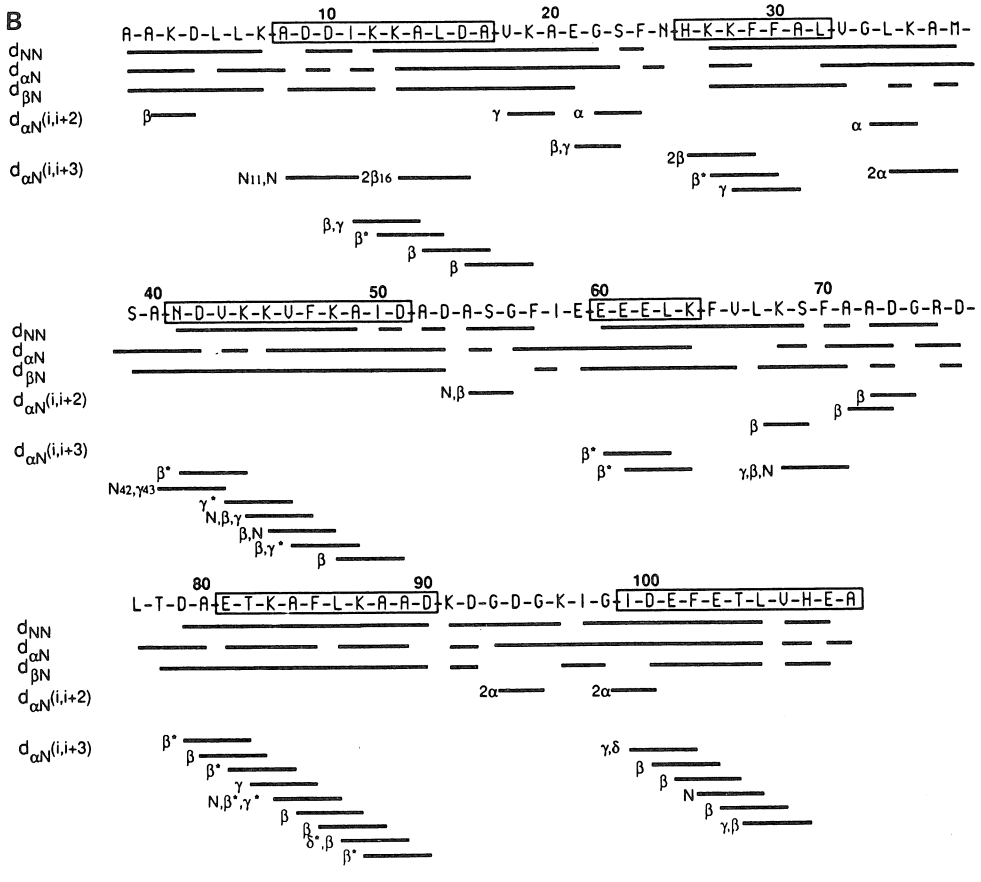


Figure 5 (continued). (b) Sequential and medium range NOEs in parvalbumin obtained from a 3D NOE-NOE spectrum (R. Boelens).

## DISCUSSION OF DR. BOELENS' PAPER (E.R.P. Zuiderweg)

It was re-emphasized that the first 2D spectrum of the single scan 3D NOE-NOE spectrum contained hardly any peaks, while the sensitivity of the resulting 3D spectrum was quite acceptable. This illustrates the multiplexing procedure in 3D NMR very nicely; the sensitivity of the experiment is determined by the total number of scans. Furthermore, it was emphasized that it is therefore hazardous to compress data before all processing is done; when doing so information can be discarded by that process.

Dr. Boelens indicated that the protein concentration used for the non-selective homonuclear 3D experiments is around 5 mM.

Dr. Boelens made the general point that the labeling necessary for heteronuclear NMR is expensive, and that in many cases it is not a straightforward process. Especially in eukaryotic systems, where post-processing may be necessary, the labeling becomes even more of a challenge. Dr. Boelens also indicated that very good homonuclear 3D NMR spectra were obtained from DNA and carbohydrates; labeling of such systems is extremely difficult.

A general discussion developed about molecular weight limitations for NMR structure determination. Dr. Kay indicated that the question revolves around the necessity of experiments; if one can do without correlated information through the backbone, very high molecular weight proteins may be tackled; it is too early to come to a conclusion on these matters. Dr. Jardetzky made the comment that larger systems have been successfully studied with NMR (Trp repressor). Trp repressor dimer is over 25 kDa and has been studied using selective deuterium labeling. Dr. Jardetzky anticipated that much larger systems can be studied if these labeling methods are combined with heteronuclear 3D NMR.

Smaller systems may also benefit from 3D NMR and isotopic labeling since much overlap occurs in the spectra of such molecules as well. Dr. Zuiderweg indicated that a large amount of overlap became apparent in the 3D spectrum of C5a (a small protein, 8.5 kDa) once it was labeled with $^{15}N$. It was also brought up by Dr. Kay that a project involving a 39 a.a. protein fragment would have been easier if $^{15}N$ labeling would have been available.

Dr. Boelens was asked how one could tell that cross peaks in the 3D NOE-NOE spectra are due to sequential interactions. Dr. Boelens indicated that a statistical approach is needed to do a reliable assignment from NOE-NOE spectra, and that work along those lines is in progress.

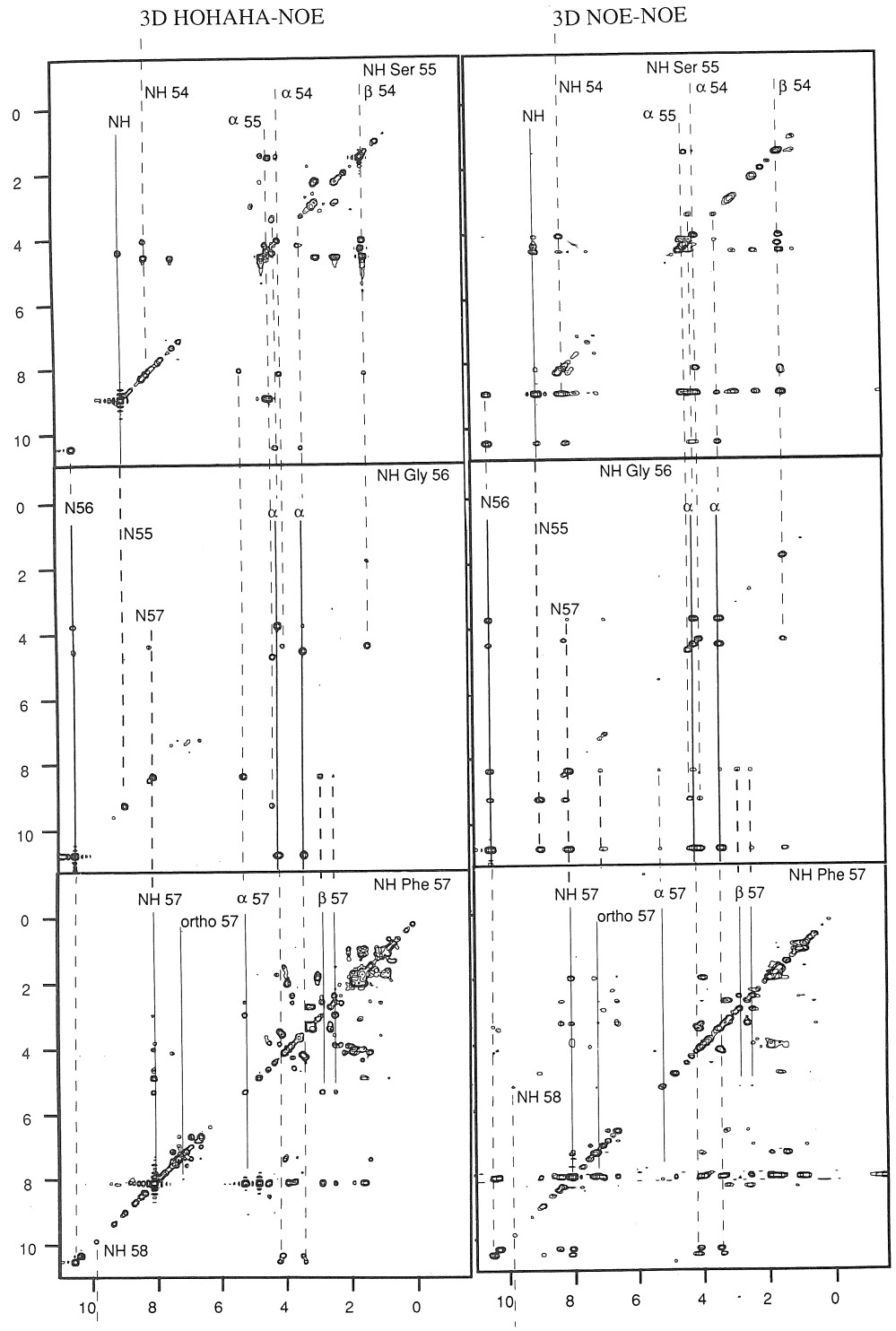


Figure 6. Cross sections through a 'clean' 3D HOHAHA-NOE and a 3D NOE-NOE spectrum of parvalbumin. Corresponding cross sections are shown from Ser 55 to Phe 57. Solid lines indicate the spin system (NH,$C^{\alpha}H$,$C^{\beta}H$ frequencies) linked to the NH frequency of the cross section. Dashed lines indicate frequencies of neighbouring (sequential and medium-range) spin systems. The 3D HOHAHA-NOE spectrum was recorded with 4 scans at 500 MHz with a 'clean' HOHAHA pulse sequence of 44 ms including trim pulses and a NOE mixing time of 150 ms. The 3D NOE-NOE spectrum was recorded with 8 scans and 2 dummy scans at 500 MHz with two identical mixing times of 150 ms (R. Boelens).

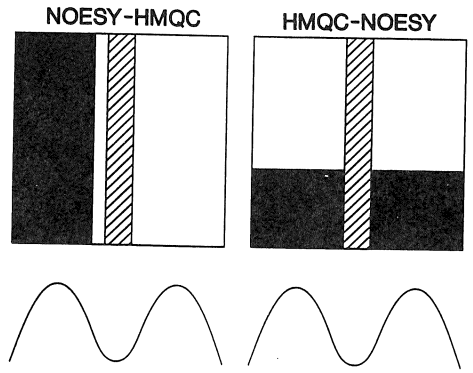


Figure 7. Comparison of the experimental artifacts observed in the NOESY-HMQC and HMQC-NOESY experiment. In NOESY-HMQC, the magnetizations, beared by any kind of protons (during $t_1$) are transferred by n.O.e. to the NH (detected during $t_3$), after its $^{15}$N labelling during $t_2$. In HMQC-NOESY, the NH magnetizations, identified during $t_1$, are $^{15}$N labelled during $t_2$, and then transferred to all protons. The regions of interest (NH-C$^{\alpha}$H, NH-C$^{\beta}$H correlation are shown as a black rectangle, and the noise artifacts during to the intense water correspond to the hatched area. In this respect, the NOESY-HMQC experiment is more suitable for protein studies. Furthermore, a frequency-selective excitation such as a 1-1 pulse (lower part of the figure) can be conveniently implemented for this option (D. Marion).

## PRACTICAL CONSIDERATIONS FOR OPTIMIZING $^{15}$N NOESY- OR HOHAHA-HMQC SPECTRA (D. Marion)

### *Optimization of Spectral Windows*

3D experiments are made up from the combination of two 2D pulse sequences: for instance, in $^{15}$N-resolved NOESY or HOHAHA 3D experiments, a homonuclear experiment is merged with a HMQC. As a result, two schemes can be devised, with either the HMQC or the homonuclear part (NOESY or HOHAHA) at the beginning of the sequence[7,8,26]. Whereas NOESY-HMQC and HMQC-NOESY are theoretically strictly equivalent, they differ in practice with regard to the location of various experimental artifacts, such as ($t_1$, $t_2$) noise and water residual signal. In fact, $^{15}$N-resolved NOESY or HOHAHA spectra of $^{15}$N-labelled proteins can only be recorded in $H_2O$, and one has therefore to cope with the suppression of the large water signal. For these reasons, the optimal compromise for recording these spectra make use of the NOESY- or HOHAHA-HMQC pulse sequence, where the amide proton chemical shift is sampled during the $t_3$ detection period (*cf.* Fig. 7).

Whereas this choice permits the easy observation of NH to C$_{\alpha}$H connectivities in an artifact-free area of the spectrum, it exhibits severe drawbacks, as far as digital resolution is concerned. During $t_3$ (where a increase of the digital resolution is almost free of charge), only a limited range of chemical shift (say from 5.5 to 10.5 ppm) has to be detected, as opposed to $t_1$ where



the entire $^1$H shift range has to be sampled. Consequently, various tricks have been implemented in order to maximize the digital resolution. During the $t_1$ period, the carrier has to be in the middle of the proton spectrum, and during the $t_3$ period, in the middle of the NH region. This carrier shifting can be achieved either by an actual change of the synthesizer frequency (with phase coherence) or by more sophisticated NMR tricks. If the TPPi method[27] is used for the quadrature detection during $t_1$, the usual $\pi/2$ phase increment can be changed into a different value, leading to a shift not equal to SW/2. For hypercomplex data[28], the same result can be achieved using a linear time-dependent phase correction of the free induction decay, before FT. Moreover, the second solution is more convenient, because the amount of shift can anyhow be adjusted after the data collection, as opposed to the TPPi case.

These methods make it possible to center the spectral windows during $t_1$ and $t_3$ independently, and the spectral width can be squeezed to a maximum. Let us point out an additional way of increasing the digital resolution, only for hypercomplex data: If the first increment in $t_2$ (the $^{15}$N dimension) is set in order to yield a 180° linear phase correction across the spectral width, the folded resonances will appear with opposite phase relative to the unfolded one making them easily identified. However, use of extensive folding may lead to signal cancellation of resonances with opposite sign. This method is not advisable in any of the proton dimensions, since baseline distortion will show up due to the immense diagonal peaks.

### *Processing of 3D NMR Spectra*

Using spectrometers designed for 2D NMR, a 3D data set appears as several files (typically 64 or 128) recorded with different timing. For instance, for each $t_2$ value, a pair of ($t_1$, $t_3$ ) files are collected for a NOESY-HMQC 3D spectrum. Therefore, a straightforward manner of processing these data can rely on any commercially available software, for the $F_1$ and $F_3$ Fourier transform, supplemented by additional software for the $F_2$ FT. A prerequisite for this simple approach is an adequate format for the data storage. A software package has been written in a modular form by Kay, Marion, and Bax[26] for the $F_2$ Fourier transformation, as well as for the pre- and post-processing routines: all manipulations, that would normally be applied to a single data point in a one dimensional process, have been converted for plane processing.

The very first step involves the windowing of the data — each ($t_1$, $t_3$) plane is scaled by a constant factor — and the window function is designed to avoid too low a weighting factor for the last $t_2$ increments, at the expense of a rather small increase of truncation artifacts. Zero-filling is merely achieved by the creation of files, which only contain zeroed data

points. The Fourier transform is a modified version of the 1D FFT for a set of N points, where N is a power of two. During its first step (the bit reversal routine), the reshuffling amounts to renaming the planes, without moving the data. The second step (the so-called butterfly algorithm) is a series of linear combination of planes: two planes are loaded from the disk, combined and then written again. As a result, the FT is done in place and the file structure (dictated by the choice of commercial software) is preserved.

Due to their size, 3D data cannot be interactively phased. In fact, with the exception of the detection dimension ($t_3$) where the hardware interferes with the phase problem (the zero order term originates from hardware phase shift, and the first order from filter time response), the required phase correction can be easily computed from the pulse sequence timing. The linear phase corrections are exclusively due to the finite duration of the pulses, during which the spins start processing. As a matter of fact, during a 90° pulse, the spins exhibit the same dephasing as during a delay of $2/\pi$ of its duration[2]. This simple rule can be used in order to compute the first-order term of the phase correction (the zero-order, as defined in the center of the spectrum, is zero). Let us point out that the time-domain phase correction (for carrier shifting) must be taken into account for computing the phase correction parameters. Here again, the $t_2$ phase correction amounts to a combination of planes, and is performed in place. The flexibility of this software has been shown recently on 4D NMR, where the 2 additional dimensions have been processed with no modification: files have to be renamed between the two processings.

*Display of 3D NMR Data*

$^{15}$N-resolved NOESY or HOHAHA spectra are conveniently displayed as $^{1}$H-$^{1}$H contour plots, since the $^{15}$N chemical shift is of no major concern, except for resolving overlaps. In fact, due to the large number of planes, there is a need for automation, and a laser printer can be used overnight for plotting the data. Handling of 64 or 128 sheets of paper for data interpretation is rather tedious, although most of the information is contained in rather limited areas of the spectrum. The 3D data can be compressed back into a 2D spectrum, by extracting strips along $F_1$ at the various chemical shifts of the amide pairs ($F_3 = ^{1}$H and $F_2 = ^{15}$N) (see Fig. 8 and Driscoll et al.[29]). Once the strips have been sequentially ordered, this data representation permits to back up the assignment by comparison of the peak patterns, principally of the $C^{\beta}$ protons.



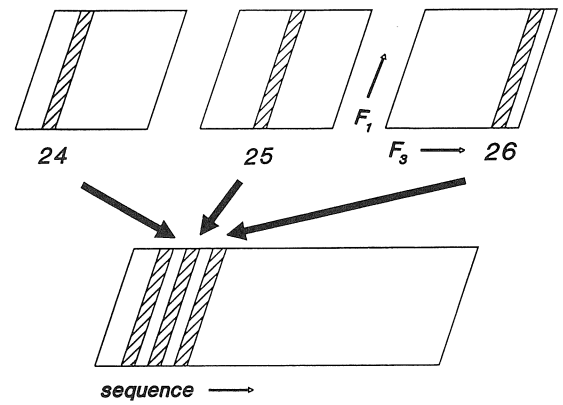


Figure 8. Data reduction for 3D NMR. Once the $^{15}$N and $^{1}$H frequencies of each amide group have been tabulated, strips running parallel to $F_1$ can be extracted by software in order to build a 2 spectrum. The strips are ordered arbitrarily before assignment and according the sequence after assignment (D. Marion).

## DISCUSSION OF DR. MARION'S PAPER (E.R.P. Zuiderweg)

The question was raised how maximum entropy processing compared with linear prediction. Dr. Marion indicated that in his hands maximum entropy processing was more robust, and that he successfully applied it to process the indirect proton domain in a 3D NOESY-HMQC experiment.

The techniques described by Dr. Marion are geared towards minimizing the required data space. The question was raised by the moderator whether the acquisition of more data points at a higher sampling rate during detection (oversampling[30]) would not be advantageous (for dynamic range). Dr. M. Delsuc, co-author on a paper on this subject, indicated that the impact of oversampling is dependent on the make of the spectrometer and that it has to be determined case-by-case whether it is worth the burden of additional data.

Data table compression was discussed. Dr. Marion indicated that he processed with MEM only the (proton) columns containing signal for the last transform of the NOESY-HMQC data. This could be done because the diagonal shows where the cross peaks are to show up.

## A NOVEL APPROACH FOR SEQUENTIAL ASSIGNMENT OF LARGER PROTEINS: TRIPLE RESONANCE THREE-DIMENSIONAL NMR SPECTROSCOPY (L.E. Kay)

Complete assignment of the backbone proton resonances of proteins forms the basis for both detailed structural and dynamical studies by NMR. Traditionally, this is carried out by relying on both through-space and through-bond connectivities provided by homonuclear NOESY and HOHAHA/TOC-

SY spectra[1]. While feasible for small proteins (< 10 kD), this approach does not yield unambiguous assignments for larger molecules due to extensive overlap and decreasing sensitivity of experiments relying on through bond proton magnetization transfer.

The limitations described above can be overcome by novel 3D heteronuclear triple resonance experiments which exploit the relatively large one-bond J couplings between the backbone $^{13}C$ and $^{15}N$ nuclei and between the backbone protons and the $^{15}N$ and $^{13}C$ nuclei to which they are directly attached[16,17]. The new experiments yield spectra almost free of overlap that provide sufficient information to obtain complete sequential backbone resonance assignments in a manner completely independent of the secondary structure of the protein under investigation. Because magnetization transfers often involve carbonyl or nitrogen spins having linewidths of only 4-8 Hz for proteins in the 15-20 KD molecular weight regime the sensitivity of the experiments is high.

Fig. 9 shows the four novel 3D pulse schemes developed to assign backbone resonances in proteins. The first 3D experiment, HNCO, correlates NH and $^{15}N$ chemical shifts of an amino acid with the carbonyl chemical shift (C′) of the preceeding residue, thereby providing valuable sequential connectivity information. The second experiment, HNCA, correlates the NH and $^{15}N$ chemical shifts with the intra-residue $C^{\alpha}$ chemical shift. In addition, a correlation between the NH and $^{15}N$ spins and the $C^{\alpha}$ spin of the preceeding residue is often observed due to the two-bond $^{15}N$-$^{13}C^{\alpha}$ coupling. In these favorable cases, a second source of sequential connectivity information is obtained. The third experiment, HCACO provides information relating to intra-residue connectivity by correlating the $H^{\alpha}$, $C^{\alpha}$ and C′ chemical shifts. Finally, the HCA(CO)N experiment provides sequential connectivity information by relating the $H^{\alpha}$ and $C^{\alpha}$ shifts with the $^{15}N$ shift of the subsequent residue.

Analysis of a HOHAHA-HMQC[31] spectra can also be extremely useful in the sequential assignment process. When combined with the HNCA experiment, the HOHAHA-HMQC experiment firmly establishes intraresidue correlations between pairs of $^{15}N$-NH and $C^{\alpha}$-$H^{\alpha}$ backbone resonances, despite significant overlap present in the 1D $^{15}N$, $^{13}C$ and $^{1}H$ spectra. Once $C^{\alpha}$-$H^{\alpha}$ pairs are obtained, the intra-residue C′ chemical shift is determined from the HCACO experiment. The NH, $H^{\alpha}$, $^{15}N$, $C^{\alpha}$ and C′ shifts from a

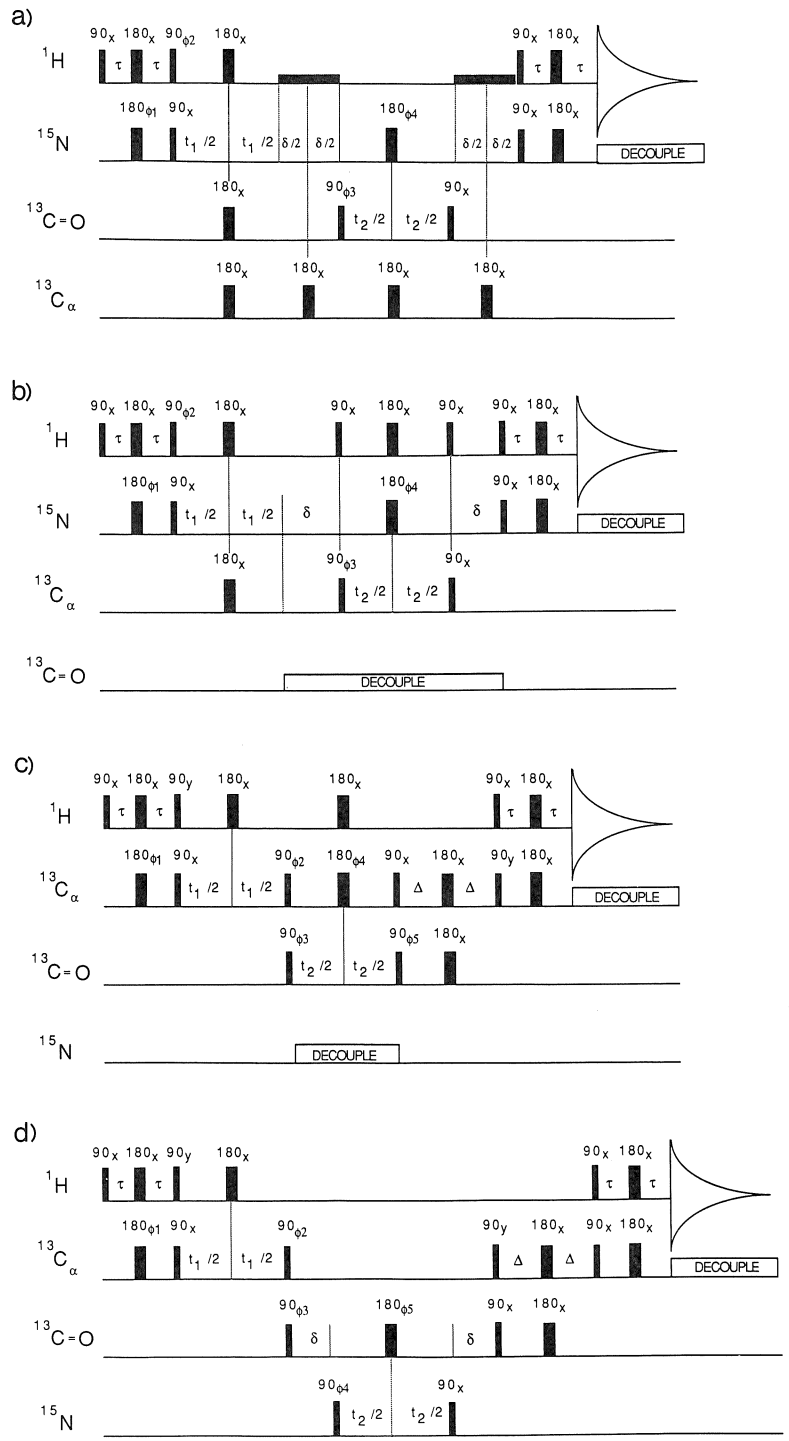


Figure 9. Pulse sequences of (a) the HNCO experiment, (b) the HNCA experiment, (c) the HCACO experiment and (d) the HCA(CO)N experiment. For schemes a and b, $H_2O$ presaturation is used and in addition, in (a) low-power water irradiation is used during the intervals delta (solid bars). The mechanism of the experiments as well as details such as the phase cycling employed and the implementation of the methods on modern spectrometers can be found in ref. 17 ( L.E. Kay).

particular residue are subsequently linked using the HCA(CO)N and HNCO spectra together with the HNCA spectrum in those cases where a sequential correlation is observed.

Fig. 10 illustrates the resolution and sensitivity that can be obtained by these methods. Several slices from five separate 3D NMR spectra recorded for the protein calmodulin (MW 16.7 KD) are presented. Fig. 10A is a region of the (C′,NH) slice taken from the HNCO spectrum at an $^{15}N$ frequency of 117.4 ppm, establishing a correlation between the NH and $^{15}N$ chemical shifts of Lys-21 and the C′ shift of Asp-20. Fig. 10B is part of the corresponding slice of the HNCA spectrum, identifying the Lys-21 $C^{\alpha}$ chemical shift. The corresponding slice from the $^{15}N$ HOHAHA-HMQC spectrum identifies the $H^{\alpha}$ chemical shift of Lys-21 (Fig. 10C). A knowledge of the $H^{\alpha}$ and $C^{\alpha}$ chemical shifts establishes the intra-residue C′ shift using the HCACO spectrum shown in Fig. 10D. The $^{15}N$ chemical shift of the subsequent residue, Asp-22, is obtained from the HCA(CO)N spectrum (Fig. 10E). Finally, a knowledge of the C′ chemical shift of Lys-21 and the $^{15}N$ shift of Asp-22 enables the assignment of the HN shift of Asp-22 from the HNCO spectrum of Fig. 10F. In this fashion all of the backbone resonances of Lys-21 have been assigned and the connection between Lys-21 and Asp-22 is thoroughly established. Note that the slice of Fig. 10G shows a weak two-bond connectivity between the Asp-22 amide nitrogen and the $C^{\alpha}$ carbon of Lys-21, providing yet another confirmation of the connectivity between Lys-21 and Asp-22.

The sequential assignment approach outlined above provides a very powerful and direct method for analyzing the NMR spectra of proteins that can be isotopically enriched with $^{15}N$ and $^{13}C$. The sensitivity of the new pulse schemes presented is sufficient to permit the recording of a 3D spectrum with a high signal to noise ratio in less than 2 days for protein concentrations in the 1 mM range. Because the spectral regions of interest are usually rather limited in any given dimension, data matrices are quite small, typically between 2-8 Mword, depending on the type of experiment. The approach described, together with 4D NMR spectroscopy[15], should enable the determination of high resolution solution structures for proteins up to at least 200 amino acids in an automated fashion.

## DISCUSSION OF DR. KAY'S PAPER (E.R.P. Zuiderweg)

The question was asked whether it would be desirable to go to even higher dimensions in these experiments. Dr. Kay indicated that that depends on the system; if lower dimensionality yields the necessary resolution, it would be easier to pick the peaks and integrate. For systems of higher molecular weight than 17 kDa, four-dimensional NMR may be necessary, in conjunc-



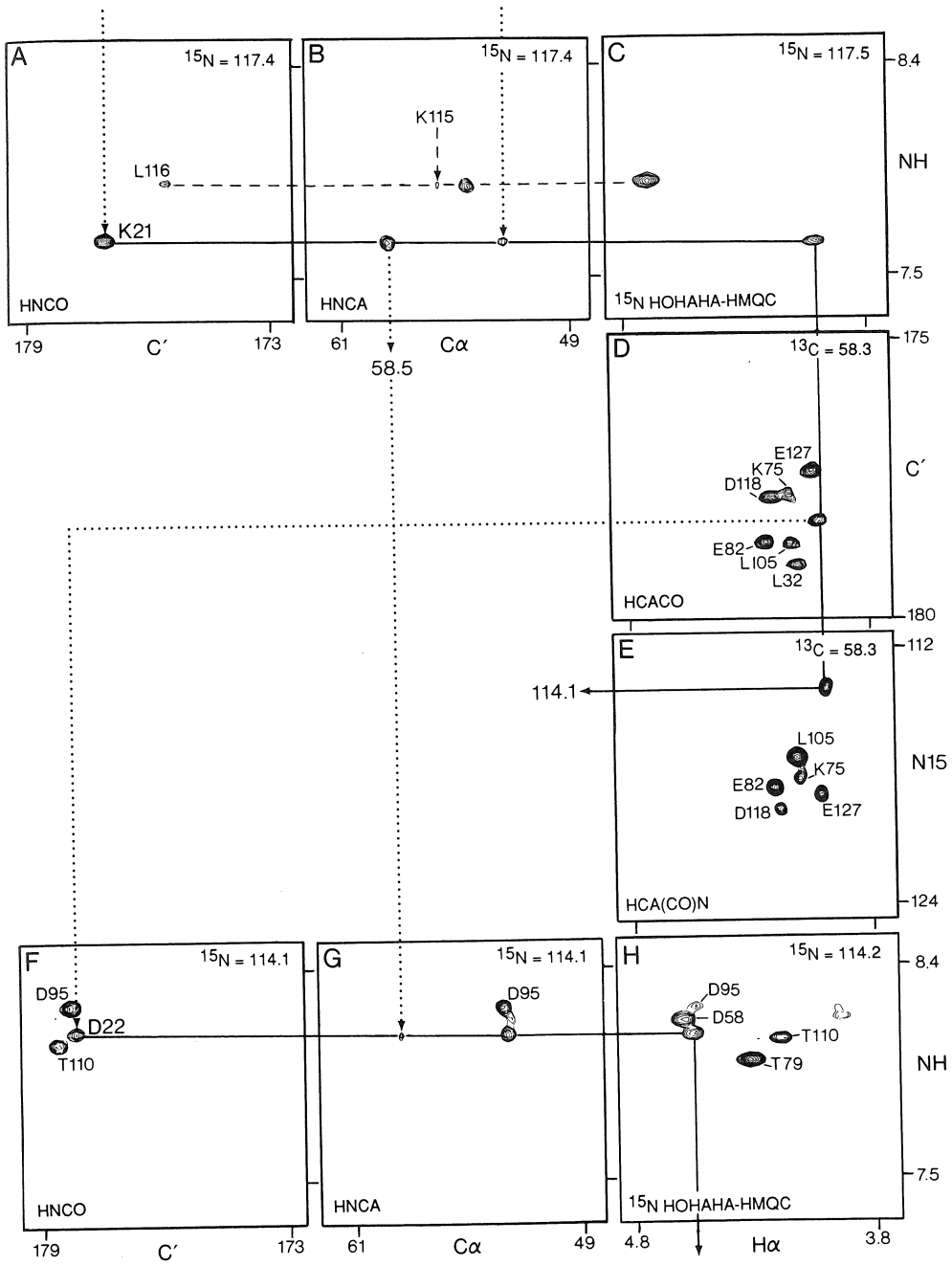


Figure 10. Selected regions of slices from five separate 3D NMR experiments discussed in the text. These regions illustrate the J correlations between Lys-21 and Asp-22. Solid and dotted lines trace the connectivity patterns for these two residues. The broken lines correspond to parts of the connectivity patterns observed for other residues (L.E. Kay).

tion with automated analysis. The problem of resolution in 4D NMR was addressed. Dr. Kay suggested to use multiple folding of the spectra in the different domains and to use a computed linear phase shift (180°) to be able to distinguish between folded and non-folded resonances (see also Dr. Marion's paper). Furthermore, it is extremely useful to use linear prediction; in fact, Dr. Kay has been experimenting with predicting 8 complex points out to 16. The experience is that sometimes negative $T_2$ values were created (interferogram increases in amplitude); but that these effects were dealt with by the apodization function and by "root reflection". The question was raised why it would be necessary to transform the predicted data; why is it not sufficient to use a table of coefficients. Dr. Kay indicated that that was a very interesting possibility. However, the approach of transforming was chosen because it would then be possible to go back and inverse transform another indirect dimension and repeat the linear prediction process.

Upon question, Dr. Kay indicated that it was necessary to have at least three channels on a spectrometer which can be phase cycled independently. More channels would give more capacities (C=O treated independently from the rest of the carbon spectrum), and the number of experiments would certainly be expanded.

## SUMMARY AND SOME UNDISCUSSED POINTS (E. R. P. Zuiderweg)

The contributors to the session have addressed several aspects of 3D NMR. It was shown that homonuclear 3D experiments can be quite powerful for solving assignment problems in not too large proteins. The cost and availability aspect of heteronuclear 3D NMR was brought forth, but consensus was that the applicability of these experiments is such that people, time and money investments for the labeling are well worth it. It was indicated that not all labeling can be easily carried out in *E. coli*; plasmid rejection in minimal media as well as folding problems of proteins in these organisms necessitate the development of labeling procedures in other organisms.

Consensus was that the novel heteronuclear techniques would in principle enable biomacromolecules up to 25,000 kDa to be studied successfully; for larger systems additional dimensions (with a concommitant loss of approximately a factor of two in sensitivity per dimension when transfers are 100% effective) or additional selective labeling need to be considered to handle the broader lines. More dimensions or higher resolution in 3D NMR imply that hardly any phase cycling can be done per indirect time increment combination. The feasibility of that approach is demonstrated in Dr. Boelens paper. In order for these fast experiments to work properly, very high standards of rf reproducibility are required from the current and future equipment, and



the unavailabilty of time for phase cycling of e.g., 180° pulses necessitates short pulses. Clearly, many channels are needed on the new spectrometers and a need for faster and/or higher resolution digitizers is emerging to cope with the large dynamic range associated with the spectra of large molecules. 3D NMR is also useful for the study of smaller molecules; it is anticipated that a significant increase in the precision of 3D structure determinations can be achieved for such molecules when overlap problems in the spectra are resolved by 3D NMR for such systems as well. No consensus was reached on the best protocol for the NMR study of larger systems. Homonuclear experiments as NOE-HOHAHA[5,6], NOE-NOE[10], heteronuclear experiments as $^{15}N$ and $^{13}C$ resolved NOESY and HOHAHA[7–9,13,14,31], $^{13}C$-$^{13}C$ coherence transfer[11,12], as well as the through-bond assignments[16,17] are all useful.

## ACKNOWLEDGEMENTS

R.B. is thankful for the collaboration with Drs. G.W. Vuister, G.J. Kleywegt, R. Kaptein (U. Utrecht) and Dr. A. Padilla (CNRS, Montpellier, Fr.). D.M. and L.E.K. thank Drs. A. Bax and M. Ikura (NIH) for their collaborations. L.E.K. would like to acknowledge the Medical Research Council of Canada for providing financial support. E.R.P.Z. acknowledges the collaboration with Drs. S.W. Fesik and E.T. Olejniczak in the 3D project at Abbott Laboratories.

## REFERENCES

1. K. Wüthrich, "NMR of Proteins and Nucleic Acids", Wiley, New York (1986).
2. R. R. Ernst, G. Bodenhausen, and A. Wokaun, "Principles of Nuclear Magnetic Resonance in One and Two Dimensions" Clarendon Press, Oxford (1987).
3. C. Griesinger, O. W. Sørensen, and R. R. Ernst, *J.Am. Chem. Soc.* **109**, 7227 (1987).
4. [a] H. D. Plant, T. H. Mareci, M. D. Cockman, and W. S. Brey, "27$^{th}$Experimental NMR Conference, Maryland, April 13-17, 1986".
   [b] G. W. Vuister and R. Boelens *J. Magn. Reson.* **73**, 328 (1987).
5. H. Oschkinat, C. Griesinger, P. J. Kraulis, O. W. Sørensen, R. R. Ernst, A. M. Gronenborn, and G. M. Clore, *Nature* **332**, 374 (1988).
6. G. W. Vuister, R. Boelens, and R. Kaptein, *J. Magn. Reson.* **80**, 176 (1988).
7. S. W. Fesik and E. R. P. Zuiderweg, *J. Magn. Reson.* **78**, 588 (1988).
8. D. Marion, L. E. Kay, S. W. Sparks, D. A. Torchia, and A. Bax, *J. Am. Chem. Soc.* **111**, 1515 (1989).
9. E. R. P. Zuiderweg, and S. W. Fesik, Biochemistry **28**, 2387 (1989).
10. R. Boelens, G. W. Vuister, T. M. G. Koning, and R. Kaptein, *J. Am. Chem. Soc.* **111**, 8525 (1989).
11. S. W. Fesik, H. L. Eaton, E. T. Olejniczak, E. R. P. Zuiderweg, L. P. McIntosh, and F. W. Dahlquist, *J.Am. Chem. Soc.* **112**, 886 (1990).
12. L. E. Kay, M. Ikura, and A. Bax, *J. Am. Chem. Soc.* **112**, 88 (1990).
13. M. Ikura, L. E. Kay, R. Tschudin, and A. Bax, *J. Magn. Reson.* **86**, 204 (1990).

14. E. R. P.Zuiderweg, L. P. McIntosh, F. W. Dahlquist, and S. W. Fesik, *J. Magn. Reson.* **86**, 210 (1990).
15. L. E. Kay, G. M. Clore, A. Bax, and A. Gronenborn, *Science* **249**, 411 (1990).
16. M. Ikura, L. E. Kay, and A. Bax, *Biochemistry* **29**, 4659 (1990).
17. L. E. Kay, M. Ikura R. Tschudin, and A. Bax, *J. Magn. Reson.* **89**, 496 (1990).
18. C. Griesinger, O. W. Sørensen, and R. R. Ernst, *J. Magn. Reson.* **84**, 14-63 (1989).
19. K. Nagayama, T. Yamazaki, M. Yoshida, S. Kanaya, H. Nakamura, Poster at NATO workshop, Il Ciocco, Italy (1990).
20. C. Griesinger, O. W. Sørensen, and R. R. Ernst, *J. Magn. Reson.* **73**, 574 (1987).
21. R. Boelens, G. W. Vuister, A. Padilla, G. J. Kleywegt, P. de Waard, T. M. G. Koning, and R. Kaptein, R. *in* "Biological Structure," Dynamics, Interactions and Expression." *Proceeding of the Sixth International Conversation in Biomolecular Stereodynamics*, R. H. Sarma and M. H. Sarma, eds., pp. 63-81, Adenine Press, New York, (1990).
22. G. W. Vuister, A. Padilla, R. Boelens, G. J. Kleywegt, and R. Kaptein, *Biochemistry* **29**, 1829 (1990).
23. A. Padilla, G. W. Vuister, R. Boelens, G. J. Kleywegt, and R. Kaptein, *J. Amer. Chem. Soc. 112*, 5024 (1990).
24. C. Griesinger, G. Otting, K. Wüthrich, and R. R. Ernst, *J. Am. Chem. Soc.* **110:**7870 (1988).
25. J. N. Breg, R. Boelens, G. W. Vuister, and R. Kaptein, *J. Magn. Reson.* **87**, 646 (1990).
26. L. E. Kay, D. Marion, and A. Bax, *J. Magn. Reson.* **84**, 72 (1989).
27. D. Marion and K. Wüthrich *Biochem. Biophys. Res. Commun.* **113**, 967 (1983).
28. D. J. States, R. A. Haberkorn, and D. J. Ruben, *J. Magn. Reson.* **48**, 286 (1982).
29. P. C. Driscoll, G. M. Clore, D. Marion, P. T. Wingfield, and A. M. Gronenborn, *Biochemistry* **29**, 3542 (1990).
30. M. A. Delsuc and J. Y. Lallemand, *J. Magn. Reson.* **56**, 34 (1986).
31. D. Marion, P. C. Driscoll, L. E. Kay, P. T. Wingfield, A. Bax, A. M. Gronenborn, and G. M. Clore, *Biochemistry* **28**, 6150 (1989).



# THE ROLE OF SELECTIVE TWO-DIMENSIONAL NMR CORRELATION METHODS IN SUPPLEMENTING COMPUTER-SUPPORTED MULTIPLET ANALYSIS BY MARCO POLO

Lyndon Emsley and Geoffrey Bodenhausen
Section de Chimie
Université de Lausanne
Rue de la Barre 2
CH-1005 Lausanne, Switzerland

## ABSTRACT

Computer-supported analysis of two-dimensional correlation spectra encounters a number of obstacles which are due, in the simplest case, to insufficient digital resolution, and, in more severe cases, to fundamental ambiguities in multiplet patterns. In this paper, we discuss various strategies involving selective two-dimensional experiments that are designed to circumvent these limitations and lift ambiguities.

## INTRODUCTION

Computer-supported analysis of multiplets in two-dimensional correlation spectra can yield a great deal of information about the networks of coupled spins under investigation[1–9]. The strategy used in our MARCO POLO program[7] (*m*ultiplet *a*nalysis by *r*eduction of *c*ross peaks and *o*rdering of *p*atterns in an *o*verdetermined *l*ibrary *o*rganization) does not use any prior knowledge about the type of molecule under investigation, i.e., it can be applied even if we do not know a priori whether we are dealing with a peptide, a nucleic acid, an alkaloid, etc. This "open-mindedness" of our strategy has

This work has been supported by the Swiss National Science Foundation, by the Commission pour l'Encouragement de la Recherche Scientifique, and by Spectrospin AG, Fällanden, Switzerland.

*Computational Aspects of the Study of Biological Macromolecules by Nuclear Magnetic Resonance Spectroscopy,* Edited by J.C. Hoch *et al.,* Plenum Press, New York, 1991